

Nonlocal buckling characteristics of heterogeneous plates subjected to various loadings

Farzad Ebrahimi*, Ramin Babaei and Gholam Reza Shaghghi

Department of Engineering, Imam Khomeini international university, Qazvin, Iran

(Received June 23, 2017, Revised December 25, 2017, Accepted December 26, 2017)

Abstract. In this manuscript, buckling response of the functionally graded material (FGM) nanoplate is investigated. Two opposite edges of nanoplate is under linear and nonlinear varying normal stresses. The small-scale effect is considered by Eringen's nonlocal theory. Governing equation are derived by nonlocal theory and Hamilton's principle. Navier's method is used to solve governing equation in simply boundary conditions. The obtained results exactly match the available results in the literature. The results of this research show the important role of nonlocal effect in buckling and stability behavior of nanoplates. In order to study the FG-index effect and different loading condition effects on buckling of rectangular nanoplate, Navier's method is applied and results are presented in various figures and tables.

Keywords: buckling; functionally graded material; linear and nonlinear loading; nonlocal elasticity; Navier's method

1. Introduction

Nanoplates and their variations offer unprecedented opportunities for incorporating physics-based concepts for controlling the physical and chemical properties for developing novel devices and sensors. The structures at nanoscale such as nanobeam, nanoplate and nanotube can be identified as the consequences of molecular manipulation that are recognized as the main parts of various nanosystems and nanodevices. Because of their shape nanoplates have unique electrical, magnetic, thermal and mechanical properties. Nanoplates can be fabricated in such a way as to exploit the mechanical and electronic properties of hybrid structures (metal-metal, metal-semiconductor and metal-oxide); Layer-by-Layer deposition with soft materials for enhanced mechanical properties and are used in uncooled infrared sensors, photovoltaic, meta-materials, chem/bio sensors and receptor-free detection.

FG materials are advanced composites, which have continuously varying material composition and properties through certain dimension in the structure to achieve the desire goals. Because the fiber-reinforced composites have a mismatch in material properties across an interface of two discrete materials bonded together, there could be the severe thermal stress concentration phenomena at the interface of them. However, by gradually varying the material properties in FGMs, this problem can be avoided or reduced. Therefore, FGMs with a mixture of the ceramic

*Corresponding author, Professor, E-mail: febrahimi@eng.ikiu.ac.ir

and metal are applied to the thermal barrier structures for the space shuttles, combustion chambers and nuclear planets, etc. (Park and Kim 2006). Classical plate theory and first-order shear deformation plate theory of plates are reformulated based on nonlocal elasticity theory by Pradhan *et al.* (2011). Cheng *et al.* (2015) presented a theoretical study for the resonance frequency and buckling load of nanoplates with high-order surface stress model. The length scale effect on buckling response of a single-layer graphene sheet embedded in a Pasternak medium is investigated by Samaei *et al.* (2011). In another work, Wang and Wang (2011) extracted governing equations for the nanoscale plates with consideration of both surface effects and non-local elasticity. Thermal postbuckling and vibration response of the FG plates are investigated by Park *et al.* (2006). Pradhan and Kumar (2011) studied the size-dependent effect on the buckling response of biaxially compressed single-layered graphene sheets. Farajpour *et al.* (2011) studied the nanoscale buckling features of the rectangular plates under axial pressure due to non-uniformity in thickness. More advanced research, including buckling of plates in the different scale had been proposed by other researchers (Analooei *et al.* 2013, Naderi and Saidi 2013, Pradhan 2012). The buckling response of orthotropic graphene sheets subjected to the various linearly varying normal in-plane forces studied by Farajpour *et al.* (2012). The analytical solutions of natural frequencies in FGM nanoplate for different boundary conditions are presented by Zare *et al.* (2015). Salehipour *et al.* (2015a, b) developed a static and vibration model for the FG small-scale plates based on modified couple stress and 3-D elasticity theories and presented the closed form solutions for in-plane and out-of-plane vibration behavior of FGM rectangular small-scale plates. A computational method based on refined plate theory involving the effect of thickness stretching is proposed for the size-dependent bending, free vibration and buckling analysis of FGM nanoplate (Nguyen *et al.* 2015). Also thermal buckling of FGM nanoplates via nonlocal third order shear deformation theory is studied by Nami *et al.* (2015). Then Daneshmehr *et al.* (2015) explored the vibration behavior of size-dependent FG nanoplates with higher-order theories. Geometrical condition effect such as axisymmetric and asymmetric on buckling of FGM circular/annular plates are studied by Bedroud *et al.* (2015). Next the 3-D nonlocal bending and vibration behavior of FGM nanoplates are studied by Ansari *et al.* (2015b). In another work Ansari *et al.* (2015a) presented buckling and vibration behavior of FGM nanoplates under thermal loading in the pre-buckling domain with considering the surface stress effect. Recently, it was shown that the Young's modulus of the FG structures can vary along both the length and thickness directions. For instance, Li and Hu (2017) investigated torsional vibration of bi-directional FG nanotubes based on nonlocal elasticity theory. They (Li *et al.* 2018) also presented the nonlinear bending of a two-dimensionally FG beam.

Most recently, it has been shown that nonlocal differential elasticity based model maybe ill-posed. Of course, due to the simplification of the nonlocal differential elasticity, many works have been focused on the size-dependent behaviors based on the nonlocal differential models. More recently, it is shown that the nonlocal differential and integral elasticity based models may be not equivalent to each other and the nonlocal differential model is an approximate model (Zhu and Li 2017a, b, c).

In this manuscript, the buckling of FGM nanoplates subjected various linearly and non-linearly varying normal stresses for simply supported boundary condition are investigated. Different loading conditions are presented for the first time. Nonlocal theory and Hamilton's principle are used to extracting governing equations and Navier's method is applied to solving governing equation. The obtained results by the Navier's method have successfully agreement with researches has done in the past. The small-scale effect on the buckling loads of the FG rectangular

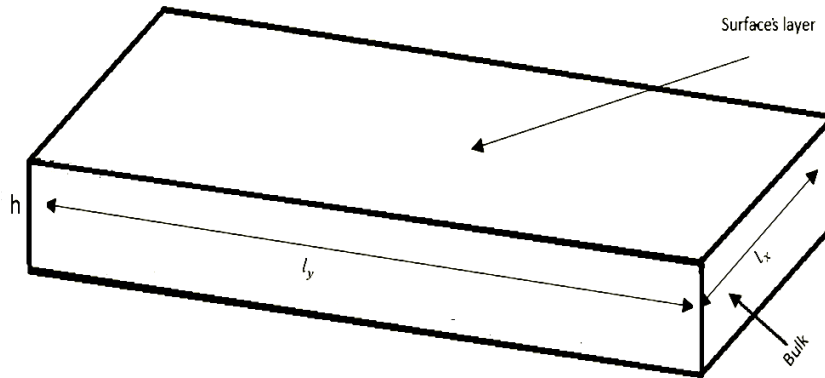


Fig. 1 Schematic view of functionally graded nanoplate

nanoplates are presented through considering various parameters such as FG-index, the length of nanoplate, numerical loading factor, nonlocal parameter, aspect ratio and mode number.

2. Formulation

2.1 Nonlocal theory

The constitutive equation of classical elasticity is an algebraic relationship between the stress and strain tensors while that of Eringen’s nonlocal elasticity involves spatial integrals which represent weighted averages of the contributions of strain tensors of all points in the body to the stress tensor at the given point (1). Though it is difficult mathematically to obtain the solution of nonlocal elasticity problems due to the spatial integrals in constitutive equations, these integro-partial constitutive differential equations can be converted to equivalent differential constitutive equations under certain conditions. So nonlocal theory is an approximate theory (Zhu and Li 2017a, b, c).

The theory of nonlocal elasticity, developed (2) states that the nonlocal stress-tensor components σ_{ij} at any point x in a body can be expressed as

$$\sigma_{ij}(x) = \int_{\Omega} (\alpha(|x' - x|, \tau) t_{ij}(x')) d\Omega(x') \tag{1}$$

where $t_{ij}(x')$ are the components of the classical local stress tensor at point x , which are related to the components of the linear strain tensor ϵ_{kl} by the conventional constitutive relations for a Hookean material, i.e.,

$$t_{ij} = C_{ijkl} \epsilon_{kl} \tag{2}$$

The meaning of Eq. (1) is that the nonlocal stress at point x is the weighted average of the local stress of all points in the neighborhood of x , the size of which is related to the nonlocal Kernel $\alpha(|x' - x|, \tau)$. Here $|x' - x|$ is the Euclidean distance and τ is a constant given by

$$\tau = \frac{e_0 a}{l} \tag{3}$$

which represents the ratio between a characteristic internal length, a (such as lattice parameter, C-C bond length and granular distance) and a characteristic external one, l (e.g. crack length, wavelength) through an adjusting constant, e_0 , dependent on each material. The magnitude of e_0 is determined experimentally or approximated by matching the dispersion curves of plane waves with those of atomic lattice dynamics. According to (2) for a class of physically admissible kernel $\alpha(|x'-x|, \tau)$ it is possible to represent the integral constitutive relations given by Eq. (1) in an equivalent differential form as

$$(1-(e_0a)\nabla^2)\sigma_{kl}=t_{kl} \quad (4)$$

where ∇^2 is the Laplacian operator. Thus, the scale length e_0a takes into account the size effect on the response of nanostructures. For an elastic material in the one dimensional case, the nonlocal constitutive relations may be simplified as (3)

$$\sigma_{xx}-\mu\frac{\partial^2\sigma_{xx}}{\partial x^2}=E\varepsilon_{xx} \quad (5)$$

where σ and ε are the nonlocal stress and strain respectively, $\mu=(e_0a)^2$ is nonlocal parameter, E is the elasticity modulus.

2.2 Functionally graded nanoplate

As depicted in Fig. 1, an FGM nanoplate of length l_x , width l_y and thickness h that is made of a mixture of ceramics and metals is considered. It is assumed that the materials at bottom surface ($Z = -h/2$) and top surface ($Z = h/2$) of the nanoplate are metals and ceramics, respectively. The local effective material properties of an FGM nanoplate can be calculated using homogenization method that is based on the Mori-Tanaka scheme. According to the Mori-Tanaka's homogenization technique, the effective material properties of the FGM nanoplate such as Young's modulus (E), Poisson's ratio (ν), mass density (ρ) and thermal extension coefficient (α) can be determined as follows (4)

$$E(z)=E_cV_c(z)+E_mV_m \quad (6a)$$

$$\rho(z)=\rho_cV_c(z)+\rho_mV_m \quad (6b)$$

$$\alpha(z)=\alpha_cV_c(z)+\alpha_mV_m \quad (6c)$$

$$\nu(z)=\nu_cV_c(z)+\nu_mV_m \quad (6d)$$

Here, the subscripts m and c refer to metal and ceramic phases. The volume fraction of the ceramic and metal phases can be defined by the power-law function as

$$V_f(z)=\left(\frac{1}{2}+\frac{z}{h}\right)^k \quad (7)$$

where k represents the power-law index. Additionally, the neutral axis of FGM nanoplate and the end supports are located on, can be determined by the following relation

$$z_0 = \frac{\int_{-(h/2)}^{(h/2)} zE(z) dz}{\int_{-(h/2)}^{(h/2)} E(z) dz} \tag{8}$$

2.3 Governing equation

u , v and w are displacements component of an arbitrary point in the mid-plane along the x , y and z directions, respectively. According to the classical theory of plate (CPT), the displacement field can be presented as

$$U = u(x, y) - z \frac{\partial W}{\partial x}, \quad V = v(x, y) - z \frac{\partial W}{\partial y}, \quad W = w(x, y) \tag{9}$$

U , V and W are the displacement components of an arbitrary point (x, y, z) at a distance z from the middle of the plane thickness in the x , y and z directions, respectively. The strain-displacement relationships are presented following strain field. These equations are independent from constitutive equations. The tensorial strain field can be written as

$$\varepsilon_{xx} = \frac{\partial u}{\partial x} - z \frac{\partial^2 W}{\partial x^2}, \quad \varepsilon_{yy} = \frac{\partial v}{\partial y} - z \frac{\partial^2 W}{\partial y^2}, \quad \varepsilon_{xy} = \frac{1}{2} \left(\frac{\partial u}{\partial y} + \frac{\partial v}{\partial x} \right) - z \frac{\partial^2 W}{\partial x \partial y} \tag{10}$$

It is important that the transverse shear deformation is negligible in the classical theory of plates. Force and moment of nonlocal elasticity are used in the obtained formulation can be presented as

$$\begin{aligned} \{N_{xx}, N_{yy}, N_{xy}\}^T &= \int_{-(h/2)}^{(h/2)} \{\sigma_{xx}, \sigma_{yy}, \sigma_{xy}\}^T dz \\ \{M_{xx}, M_{yy}, M_{xy}\}^T &= \int_{-(h/2)}^{(h/2)} \{\sigma_{xx}, \sigma_{yy}, \sigma_{xy}\}^T z dz \end{aligned} \tag{11}$$

The strain energy of the nanoplate in the presence of surface stress on the basis of the continuum surface elasticity theory can be introduced as

$$U = \frac{1}{2} \int_A \int_{-(h/2)}^{(h/2)} \sigma_{ij} \varepsilon_{ij} dz dA \tag{12}$$

The work done by the external force can be represented as follows

$$W_{ext} = \int_{-(h/2)}^{(h/2)} qwdz \tag{13}$$

Now, by using Hamilton's principle

$$\int_{t_1}^{t_2} (\delta U - \delta W^{ext}) dt = 0 \tag{14}$$

And taking the variation of w and integrating by parts as follows

$$\begin{aligned}\delta U &= \int_V \sigma_{xx} \delta \varepsilon_{xx} dv + \int_V \sigma_{yy} \delta \varepsilon_{yy} dv + \int_V \sigma_{xy} \delta \varepsilon_{xy} dv \\ &= \int_V \sigma_{xx} \delta \left(\frac{\partial u}{\partial x} - z \frac{\partial^2 W}{\partial x^2} \right) dv + \int_V \sigma_{yy} \delta \left(\frac{\partial v}{\partial y} - z \frac{\partial^2 W}{\partial y^2} \right) dv \\ &\quad + \int_V \sigma_{xy} \delta \left(\frac{1}{2} \left(\frac{\partial u}{\partial y} + \frac{\partial v}{\partial x} \right) - z \frac{\partial^2 W}{\partial x \partial y} \right) dv\end{aligned}\quad (15)$$

And for external work can be revealed

$$\delta W^{ext} = \int_A q \delta w dA \quad (16)$$

in which q is the transverse force per unit area.

The motion equation and the boundary conditions will be obtained by setting the coefficients of δw equal to zero as, motion equation obtained from the above relationships are as follows

$$\frac{\partial(N_{xx})}{\partial x} + \frac{\partial(N_{xy})}{\partial y} = 0 \quad (17a)$$

$$\frac{\partial(N_{xy})}{\partial x} + \frac{\partial(N_{yy})}{\partial y} = 0 \quad (17b)$$

$$\frac{\partial^2(M_{xx})}{\partial x^2} + 2 \frac{\partial^2(M_{xy})}{\partial x \partial y} + \frac{\partial^2(M_{yy})}{\partial y^2} + q + \frac{\partial}{\partial x} \left(N_{xx} \frac{\partial w}{\partial x} + N_{xy} \frac{\partial w}{\partial y} \right) + \frac{\partial}{\partial y} \left(N_{xy} \frac{\partial w}{\partial x} + N_{yy} \frac{\partial w}{\partial y} \right) = 0 \quad (17c)$$

And the relevant boundary condition can be related to the following formulation

$$\delta u = 0 \quad \text{or} \quad N_{xx} n_x + N_{xy} n_y = 0 \quad (18a)$$

$$\delta v = 0 \quad \text{or} \quad N_{xy} n_x + N_{yy} n_y = 0 \quad (18b)$$

$$\delta w = 0 \quad \text{or}$$

$$\left(N_{xx} \frac{\partial w}{\partial x} + N_{xy} \frac{\partial w}{\partial y} + \frac{\partial(M_{xx})}{\partial x} + \frac{\partial(M_{xy})}{\partial y} \right) n_x + \left(N_{xy} \frac{\partial w}{\partial x} + N_{yy} \frac{\partial w}{\partial y} + \frac{\partial(M_{xy})}{\partial x} + \frac{\partial(M_{yy})}{\partial y} \right) n_y = 0 \quad (18c)$$

$$\delta \left(\frac{\partial w}{\partial x} \right) = 0 \quad \text{or} \quad M_{xx} n_x + M_{xy} n_y = 0 \quad (18d)$$

$$\delta \left(\frac{\partial w}{\partial y} \right) = 0 \quad \text{or} \quad M_{xy} n_x + M_{yy} n_y = 0 \quad (18e)$$

where (n_x, n_y) denotes the direction cosines of the outward unit normal to the boundary of the mid-plane. To obtain the equation of motion should be nonlocal effect must give effect to the above equation.

According to the generalized Hook's law

$$\begin{bmatrix} \sigma_{xx} \\ \sigma_{yy} \\ \sigma_{xy} \end{bmatrix} = [Q] \begin{bmatrix} \varepsilon_{xx} \\ \varepsilon_{yy} \\ \varepsilon_{xy} \end{bmatrix} \quad (19)$$

where $[\sigma]$ and $[\varepsilon]$ are stress and strain matrix and $[Q]$ represent fourth order elasticity matrix as follows

$$[Q] = \begin{bmatrix} \frac{E(z)}{1-\nu^2} & \frac{E(z)\nu}{1-\nu^2} & 0 \\ \frac{E(z)\nu}{1-\nu^2} & \frac{E(z)}{1-\nu^2} & 0 \\ 0 & 0 & \frac{E(z)}{2(1+\nu)} \end{bmatrix} \quad (20)$$

By definition that we had in the previous section article, should we change the equation above as follows

$$\begin{bmatrix} N_{xx} \\ N_{yy} \\ N_{xy} \end{bmatrix} = [C] \begin{bmatrix} \frac{\partial u}{\partial x} \\ \frac{\partial v}{\partial y} \\ \frac{\partial u}{\partial y} + \frac{\partial v}{\partial x} \end{bmatrix} \quad (21)$$

$$\begin{bmatrix} M_{xx} \\ M_{yy} \\ M_{xy} \end{bmatrix} = [D] \begin{bmatrix} \frac{\partial^2 W}{\partial x^2} \\ \frac{\partial^2 W}{\partial y^2} \\ 2 \frac{\partial^2 W}{\partial x \partial y} \end{bmatrix} \quad (22)$$

The matrix of $[C]$ and $[D]$'s component in the above equations are defined as follows

$$C_{ij} = \int_{-(h/2)}^{(h/2)} Q_{ij} dz \quad (23)$$

$$D_{ij} = - \int_{-(h/2)}^{(h/2)} Q_{ij} z dz \quad (24)$$

Eringen's equations as follows spread

$$N_{xx} - \mu \left(\frac{\partial^2 N_{xx}}{\partial x^2} + \frac{\partial^2 N_{xx}}{\partial y^2} \right) = C_{11} \frac{\partial u}{\partial x} + C_{12} \frac{\partial v}{\partial y} \quad (25a)$$

$$N_{yy} - \mu \left(\frac{\partial^2 N_{yy}}{\partial x^2} + \frac{\partial^2 N_{yy}}{\partial y^2} \right) = C_{21} \frac{\partial u}{\partial x} + C_{22} \frac{\partial v}{\partial y} \quad (25b)$$

$$N_{xy} - \mu \left(\frac{\partial^2 N_{xy}}{\partial x^2} + \frac{\partial^2 N_{xy}}{\partial y^2} \right) = C_{33} \left(\frac{\partial u}{\partial y} + \frac{\partial v}{\partial x} \right) \quad (25c)$$

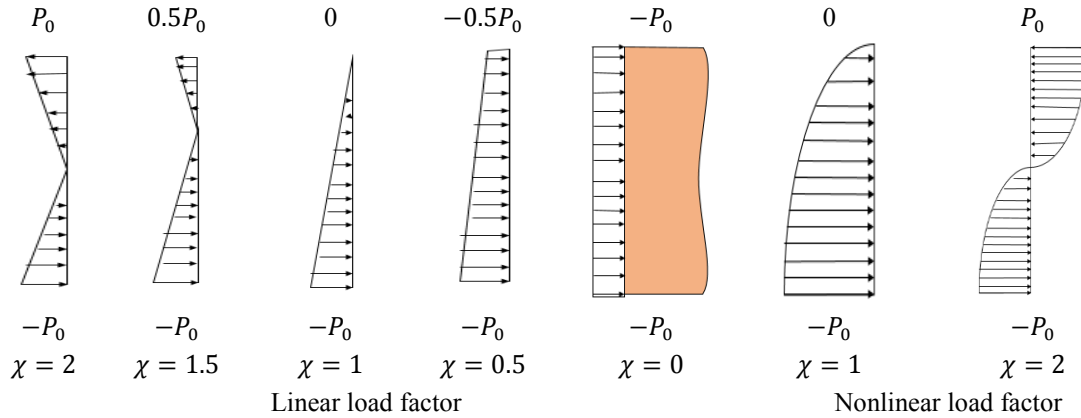


Fig. 2 Different load factor

$$M_{xx} - \mu \left(\frac{\partial^2 M_{xx}}{\partial x^2} + \frac{\partial^2 M_{xx}}{\partial y^2} \right) = -D_{11} \frac{\partial^2 W}{\partial x^2} + D_{12} \frac{\partial^2 W}{\partial y^2} \quad (25d)$$

$$M_{yy} - \mu \left(\frac{\partial^2 M_{yy}}{\partial x^2} + \frac{\partial^2 M_{yy}}{\partial y^2} \right) = -D_{21} \frac{\partial^2 W}{\partial x^2} + D_{22} \frac{\partial^2 W}{\partial y^2} \quad (25e)$$

$$M_{xy} - \mu \left(\frac{\partial^2 M_{xy}}{\partial x^2} + \frac{\partial^2 M_{xy}}{\partial y^2} \right) = -2D_{33} \frac{\partial^2 W}{\partial x \partial y} \quad (25f)$$

By inserting motion equation in the nonlocal equation, the governing equation of the nonlocal theory of plate for buckling in terms of w can be obtained as follows

$$D_{11} \frac{\partial^4 w}{\partial x^4} + 2(D_{12} + D_{33}) \frac{\partial^4 w}{\partial x^2 \partial y^2} + D_{22} \frac{\partial^4 w}{\partial y^4} + (\mu \nabla^2 - 1) \left(q + N_{xx} \frac{\partial^2 W}{\partial x^2} + 2N_{xy} \frac{\partial^2 W}{\partial x \partial y} + N_{yy} \frac{\partial^2 W}{\partial y^2} \right) = 0 \quad (26)$$

Now, we assume that the plate under the following linearly and non-linearly varying normal loads

$$N_{xx} = -P_0 \left(1 - \chi \left(\frac{y}{l_y} \right)^{1 \text{ or } 2} \right), \quad N_{yy} = 0, \quad N_{xy} = 0, \quad q = 0 \quad (27)$$

χ specifies the amount of numerical loading factors, if y is of the first order loading factor is in linearly phase and if y is of the second order loading factor is in non-linearly condition. P_0 is the compressive force per unit length at $y = 0$. This in-plane force distribution is seen at the two nanoplates opposite edges ($x = 0, x = l_x$). χ 's change shows the different form of in-plane loadings. If $\chi = 0$, then the situation of uniform compressive force is investigated. If $\chi = 1$, the force decreases from $-P_0$ at $y = 0$, to zero at $y = l_y$ and if $\chi = 2$, we'll see pure bending. These different situations of loadings condition are shown in Fig. 2. Substituting N_{xx} defined variables

into equation of motion yields the below fourth-order PDE of the nonlocal theory of the plate for buckling of functionally graded nanoplate.

$$D_{11} \frac{\partial^4 w}{\partial x^4} + 2(D_{12} + D_{33}) \frac{\partial^4 w}{\partial x^2 \partial y^2} + D_{22} \frac{\partial^4 w}{\partial y^4} - P_0 \left(\mu \left[\left(1 - \chi \frac{y}{l_y}\right) \frac{\partial^4 w}{\partial x^4} + \left(1 - \chi \frac{y}{l_y}\right) \frac{\partial^4 w}{\partial x^2 \partial y^2} \right] - \left(1 - \chi \frac{y}{l_y}\right) \frac{\partial^2 w}{\partial x^2} \right) = 0 \quad (28)$$

For create non-dimensional state of above equation, define the following parameters

$$W = \frac{w}{l_x}, \quad \xi = \frac{x}{l_x}, \quad \eta = \frac{y}{l_y}, \quad \psi = \frac{D_{12} + D_{33}}{D_{11}}, \quad \lambda = \frac{D_{22}}{D_{11}}, \quad \gamma = \frac{\mu}{l_x}, \quad \beta = \frac{l_x}{l_y} \quad (29)$$

3. Solution procedure

In order to predict solution of equation (28) analytical approach can be applied for simply support-Simply support boundary condition. In this paper, governing equation is solved by using the Navier’s approach. For the simply supported boundary condition, according to the article Aksencer and Aydogdu (2011) it can be shown that the shape function can be written in following statement double Fourier series. This approach is changing partial equation to numerical equation by inserting following shape function to governing equation.

$$w(x, y, t) = \sum_{m=1}^{\infty} \sum_{n=1}^{\infty} W_{mn} \sin\left(\frac{m\pi x}{l_x}\right) \sin\left(\frac{n\pi y}{l_y}\right) e^{i\omega t} \quad (30)$$

Because the subject matter is buckling article, time-dependent terms are deleted. And m and n are the half wave numbers. For this purpose, incorporating equation (30) into equation (28), will have

$$D_{11} \left(\frac{m\pi}{l_x}\right)^4 + 2(D_{12} + D_{33}) \left(\frac{m\pi}{l_x}\right)^2 \left(\frac{n\pi}{l_y}\right)^2 + D_{22} \left(\frac{n\pi}{l_y}\right)^4 - P_0 \left(\mu \left[\left(1 - \chi \frac{y}{l_y}\right) \left(\frac{m\pi}{l_x}\right)^4 + \left(1 - \chi \frac{y}{l_y}\right) \left(\frac{m\pi}{l_x}\right)^2 \left(\frac{n\pi}{l_y}\right)^2 \right] - \left(1 - \chi \frac{y}{l_y}\right) \left(\frac{n\pi}{l_y}\right)^2 \right) = 0 \quad (31)$$

That P_0 shows as follows

$$P_0 = \left(\mu \left[\left(1 - \chi \frac{y}{l_y}\right) \left(\frac{m\pi}{l_x}\right)^4 + \left(1 - \chi \frac{y}{l_y}\right) \left(\frac{m\pi}{l_x}\right)^2 \left(\frac{n\pi}{l_y}\right)^2 \right] - \left(1 - \chi \frac{y}{l_y}\right) \left(\frac{n\pi}{l_y}\right)^2 \right) / \left(D_{11} \left(\frac{m\pi}{l_x}\right)^4 + 2(D_{12} + D_{33}) \left(\frac{m\pi}{l_x}\right)^2 \left(\frac{n\pi}{l_y}\right)^2 + D_{22} \left(\frac{n\pi}{l_y}\right)^4 \right) \quad (32)$$

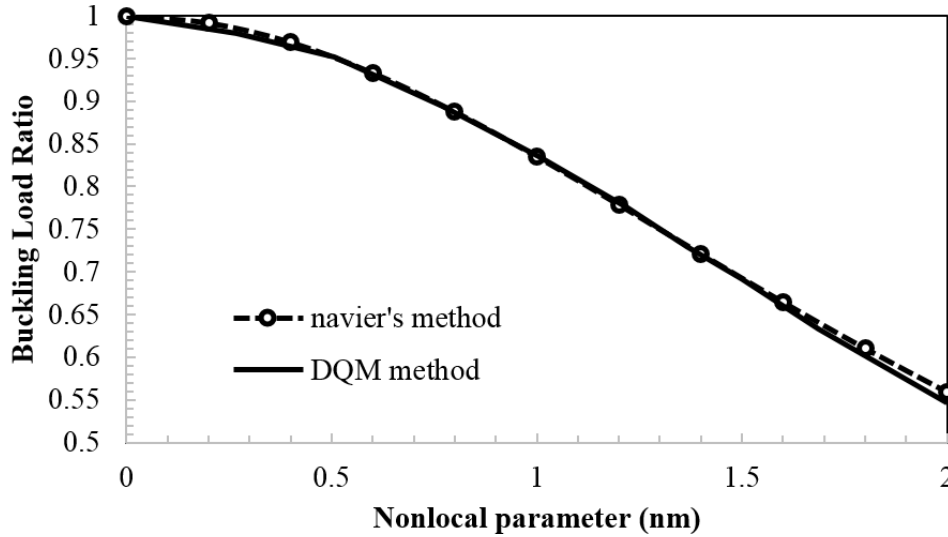


Fig. 3 Change of buckling load ratio with the nonlocal parameter for different load factors ($l_x = 10 \text{ nm}$)

It is assumed that simply supported boundary condition is in all directions.

4. Results and discussion

According to the previous studies in buckling of size dependent plates we will define the following non-dimensional parameter

$$\text{Buckling load factor} = \frac{\text{nonlocal buckling load}}{\text{local buckling load}} \quad (33)$$

Above parameter is the name of the famous buckling load ratio and it has been used in many articles (Pradhan and Murmu 2009, 2010). The present results are collation with the buckling response of square single-layered grapheme sheet (SLGS) as presented (Pradhan and Murmu 2010). This comparison can be seen in Figure 3. The nanoplate is under load by a uniformity distributed normal force from $x = 0$ to $x = l_x$. In this case, the numerical loading factor is equal to zero at ($\chi = 0$). The length of the model and y is considered 10 nm and 4 nm which boundary condition is assumed simply support. Easily visible that the results are consistent with the results Pradhan and Murmu (2010).

The plates are rectangular with the simply supported boundary condition along four edges and made of aluminum ($E=70 \text{ GPa}$) and alumina ($E=380 \text{ Gpa}$). Effectiveness of different loading conditions on nanoplate's buckling characteristics, changes non-dimensional buckling load with loading factor for simply supported boundary condition was shown in Figure 4. This figure shows, the buckling increases when the load factor increases from 0 to 2, especially for local model. Effects of various loading factor on buckling increases by decrease in amount of nonlocal parameters. For more descriptions, the nonlocal parameter effect on the buckling load is more important in the pure bending ($\chi = 2$). However, the difference between local and nonlocal buckling loads increases when the load factor increases. Change non-dimensional to nonlocal

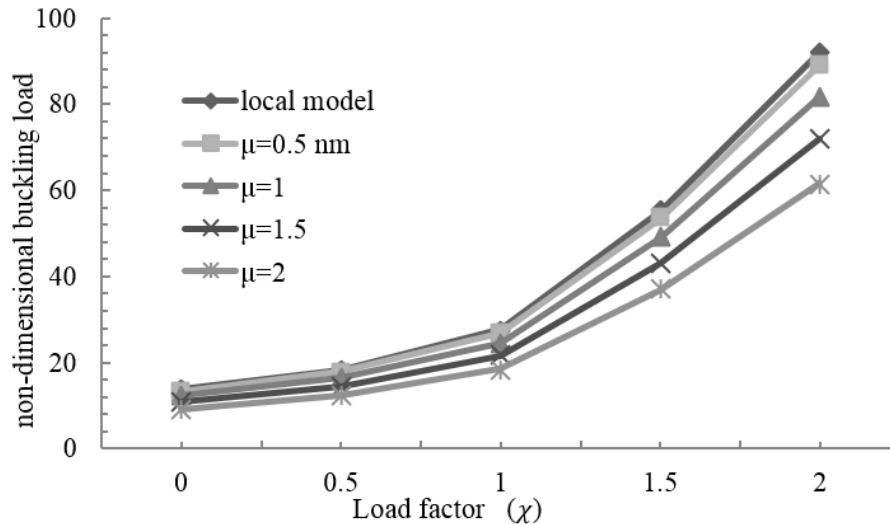


Fig. 4 The effect of different loading condition on the non-dimensional buckling load for ssss nanoplates ($\beta=0.5$ and $l_x = 10$)

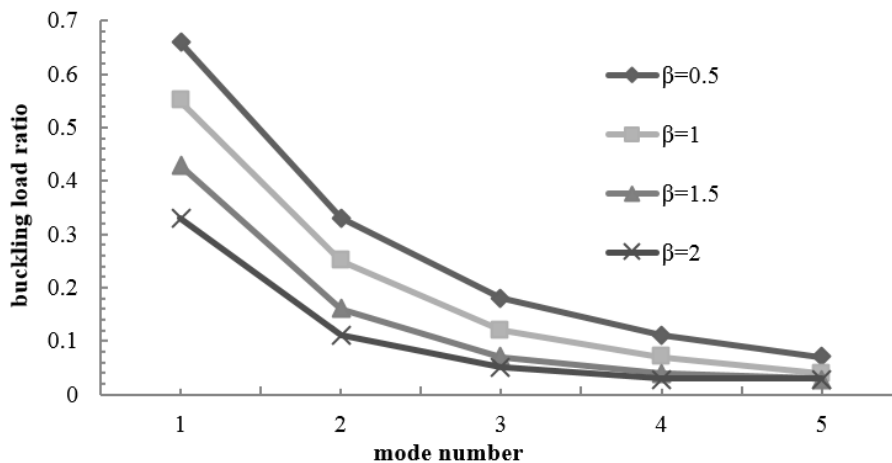


Fig. 5 Change of buckling load ratio with mode number for different aspect ratio

parameter in different loading factor can be seen in Table 1. In this table, the amount of nonlocal parameters change from 0 to 2. The table shows the non-dimensional buckling load calculated based on the nonlocal theory, are lesser than the non-dimensional buckling load calculated based on the local theory in various load factors and in all cases. In addition, non-dimensional buckling decreases as the nonlocal parameter increases and also it causes the stiffness of structure decreases in fixed side length. The non-dimensional buckling of functionally graded nanoplate when χ is 2 is bigger than other states. In addition, the amount of buckling increases when loading factor increase from 0 to 2 especially in a constant. To illustrate the small scale effect on the results of nanoplate with larger length in sides, the variations of non-dimensional with nonlocal parameter in special case ($l_x = 20 \text{ nm}$) are presented in Table 2. After that, different load factors are assumed for the rectangular functionally graded nanoplate. According to this table, it can be concluded that

Table 1 Change of non-dimensional buckling with nonlocal parameter for different load factor ($l_x = 10$)

χ	μ				
	0	0.5	1	1.5	2
0	32.9645	31.4142	27.5302	22.8265	18.4204
0.5	41.2056	39.2678	34.4128	28.5331	23.0254
1	54.9408	52.3571	45.8837	38.0442	30.7006
1.5	82.4112	78.5356	68.8256	57.0662	46.0509
2	164.822	157.071	137.651	114.132	92.1018

Table 2 Change of non-dimensional buckling with nonlocal parameter for different load factor ($l_x = 20$)

χ	μ				
	0	0.5	1	1.5	2
0	32.9645	32.5648	31.4142	29.6701	27.5302
0.5	38.7817	38.3091	36.9579	34.9060	32.3885
1	47.0921	46.5182	44.8775	42.3859	32.3989
1.5	59.9354	59.2050	57.1168	53.9457	50.0550
2	83.4112	81.4069	78.5356	74.1753	68.8256

the scale effects are lost after a special length in all cases and for various load factors. This is predictable because with the increase of dimension, the effect of nonlocal parameters decreases. Furthermore, the gap between the amounts in different loading factor piecemeal reduces with increasing nanoplate's dimension. Anyway, it is realized that the gap between pure bending with other states doesn't disappear, even for $l_x = 20 \text{ nm}$. In other words, when $\chi = 2$ then the effects of nonlocal parameters are more important than other states.

Figure 5 shows the influence of small length scale on the higher buckling modes. The variation of buckling load ratio with different mode numbers (m) and various aspect ratios (β) of functionally graded nanoplates can be seen in Figure 5. $\mu = 2$, $l_x = 10$ and $\chi = 1$ are parameters that available in this graph. The figure shows that, the amount of load ratios reduced when the mode numbers become greater in various aspect ratios. By increase in the amount of mode number, the load ratio reduced in a smooth manner phase except for $\beta = 0.5$. In other words, the size dependent effect is larger in higher modes. This event happens because in higher mode, small wavelength influence is large and important. At the small amount of wavelengths or higher mode numbers, the rate of interaction between atoms becomes larger and it causes; the size effect in fact becomes greater. It can be seen that, the difference between the curves ($\beta = 1, 1.5, 2$) in fact reduced when the mode number becomes greater. Furthermore, in Fig. 5 it can be found that the mode number becomes greater, the curves for different loading ratio gradually become flat after a special mode number. The response of this part must be expounded as the buckling mode number has not important effect in the buckling load ratio when mode numbers has steady growth ($m \geq 4$). Also, it is true for large aspect ratios (*more than 1*).

Table 3 Shows the effects of various FG Indexes and nonlocal parameter in dimensional buckling of functionally graded nanoplate. In this case same to all of other cases in this research, results are calculated for simply supported boundary condition at all edges of plate. This table includes both of linear and nonlinear various load factors. It is assumed in this table, the plate is

Table 3 Change of dimensional buckling in different linear and nonlinear loading factor, FG index and aspect ratio (μ) in $\beta = 1, l_x = 10 \text{ nm}$

Nonlocal Parameter(μ)	FG Index	Linear Load Factor (χ)					Nonlinear Load factor(χ)	
		0	0.5	1	1.5	2	1	2
0	0	0.0893	0.1117	0.1489	0.2234	0.4469	0.1064	0.1314
	2	0.3269	0.4086	0.5448	0.8172	1.6346	0.3891	0.4807
	10	0.4077	0.5096	0.6795	1.0193	2.0387	0.4854	0.5996
2	0	0.0499	0.0624	0.0832	0.1248	0.2497	0.0594	0.9734
	2	0.1826	0.2283	0.3044	0.4567	0.9334	0.2174	0.2686
	10	0.2278	0.2848	0.3797	0.5696	1.1392	0.2712	0.3350
5	0	0.015	0.0188	0.0251	0.0376	0.0753	0.0179	0.0221
	2	0.055	0.0688	0.0918	0.1377	0.2754	0.0655	0.0810
	10	0.0687	0.0858	0.1145	0.1717	0.3435	0.0655	0.1010

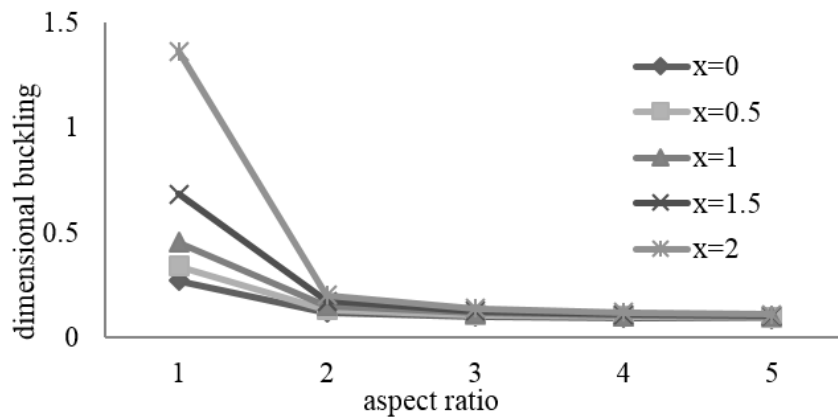


Fig. 6 The effect of different aspect ratio on the dimensional buckling load for ssss B.C in different linear load factor ($\mu = 1 \text{ nm}, l_x = 10 \text{ nm}$ and $k = 2$)

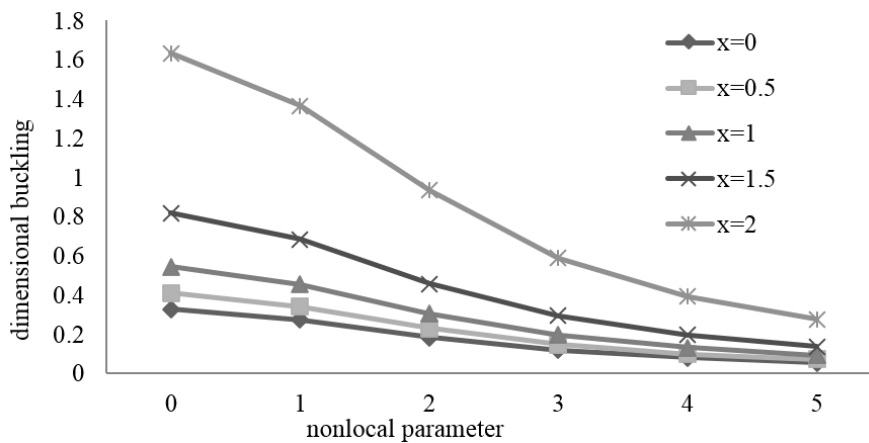


Fig. 7 The effect of different nonlocal parameter on the dimensional buckling load for ssss B.C in different linear load factor ($\beta = 1, l_x = 10 \text{ nm}$ and $k = 2$)

Table 4 Change of dimensional buckling in different linear and nonlinear loading factor, FG index and aspect ratio (β) in $\mu = 1 \text{ nm}$, $l_x = 10 \text{ nm}$

β	FG Index	Linear Load factor (χ)					Nonlinear Load Factor (χ)	
		0	0.5	1	1.5	2	1	2
1	0	0.0746	0.0933	0.1244	0.1866	0.3732	0.0888	0.1097
	2	0.273	0.3412	0.455	0.6825	1.3651	0.325	0.4015
	10	0.3405	0.4256	0.5675	0.8513	1.7026	0.4054	0.5007
2	0	0.0331	0.0368	0.0414	0.0473	0.0552	0.0345	0.036
	2	0.1211	0.1346	0.1514	0.1731	0.2019	0.1262	0.1317
	10	0.1511	0.1679	0.1889	0.2159	0.2519	0.1574	0.1642
5	0	0.0253	0.0264	0.0275	0.0288	0.0301	0.0255	0.0256
	2	0.0927	0.0965	0.1007	0.1053	0.1103	0.0932	0.0939
	10	0.1156	0.1204	0.1256	0.1313	0.1376	0.1163	0.1171

Table 5 Change of dimensional buckling load ratio in different load ratio and FG index in $\beta = 1$, $l_x = 10 \text{ nm}$ and $\mu = 1 \text{ nm}$

FG Index	Linear load factor					Nonlinear load factors	
	0	0.5	1	1.5	2	1	2
0	0.0746	0.0933	0.1244	0.1866	0.3732	0.0888	0.1097
2	0.273	0.3412	0.455	0.6825	1.3651	0.325	0.4015
4	0.3013	0.3767	0.5022	0.7534	1.5068	0.3587	0.4431
6	0.3186	0.3983	0.5311	0.7967	1.5934	0.3793	0.4686
8	0.3311	0.4139	0.5518	0.8278	1.6556	0.3942	0.4869
10	0.3405	0.4256	0.5675	0.8513	1.7026	0.4054	0.5007

square ($\beta = 1$) and the length of each edge is 10 nm . The results clearly show in each of loading factor, whether linear or nonlinear by increase in nonlocal parameter, the amount of buckling in same FG index reduced. This behavior was predictable because when nonlocal parameter becomes greater, the results are affected from all surrounding point behavior and with this increase, results will be more accurate. In addition, when FG index increases, in same case similar to above mentioned, the buckling come greater and the results are closer to real behavior.

Table 4 shows the effect of various aspect ratio and FG index in dimensional buckling of functionally graded nanoplate. Assumed conditions are similar to previous table expecting that, in this table nonlocal parameter is 1 ($\mu = 1 \text{ nm}$). The results show buckling decreases as the aspect ratio increases or the plate come thinner. This behavior is visible for all of cases. In this case, by increase in the FG index, the amount of buckling increases too. The important note in both tables is the gap between pure bending states buckling with other cases. This shows the designer could be cautious in design of structure under bending load.

Figure 7 shows a schematic for the special cases of the results of Table 3 in which it is assumed that the FG index is 2 ($k = 2$) and shows the effect of nonlocal parameters on buckling load of the square nanoplate in different linear load factor. Similarly, Figure 6 shows a schematic for the results tabulated in Table 4 in which the nonlocal parameter is assumed to be 1 ($\mu = 1 \text{ nm}$)

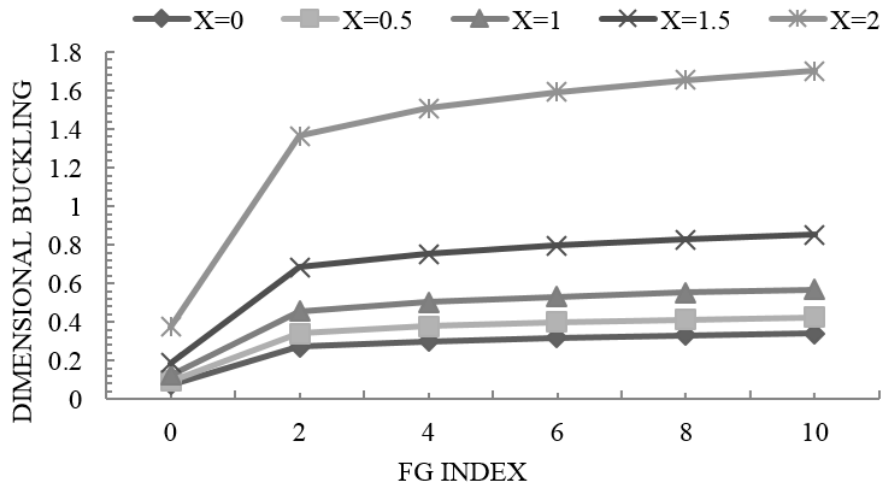


Fig. 8 Change of dimensional buckling versus FG material’s parameter in different linear load factor (χ) in $\beta = 1, l_x = 10 \text{ nm}$ and $\mu = 1 \text{ nm}$

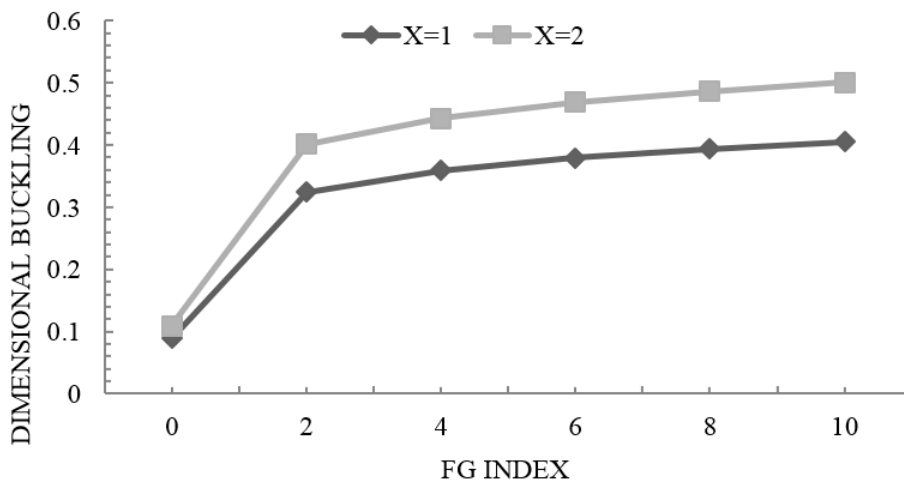


Fig. 9 Change of dimensional buckling versus FG material’s parameter in different nonlinear load factor (χ) in $\beta = 1, l_x = 10 \text{ nm}$ and $\mu = 1 \text{ nm}$

and it shows the effect of different aspect ratios on buckling load of nanoplate in different linear load factors.

Table 5 shows the response of buckling in different linearly and nonlinearly loading factor. Figure 8 and Figure 9 is a schematic of Table 5.

Figure 8 reveals the effect of FG index on the dimensional buckling load ratio of simply supported plate in different linear load factor. In this figure, it can be seen that dimensional buckling loading ratio in the FGM plate is higher than that of pure metallic plate and fundamental frequency and buckling loading increase significantly as the value of k increases. Those are because pure metallic plate has lower stiffness than FGM plate. Similarly, Figure 9 shows these details for nonlinear different load factor.

5. Conclusions

A general view of the article contains a lot of content, including the importance of size dependent effect on the buckling response of FG nanoplates subjected to linear in-plane load based on nonlocal elasticity theory. The governing equation is computed using Navier's method and related results are compared with the results of the differential quadrature method (DQM). Nonlocal buckling load are lesser than the local states for various loading conditions. In addition, buckling load ratio decreases as the nonlocal parameter increases and also the non-dimensional buckling load increases when the FG index increases. For the special case, with pure in-plane bending loading condition applied in the model, the effect of nonlocality is pronounced. It can be seen that, buckling load ratio decreases as aspect ratio increases. Further, it is visible that the effect of small scale parameter increases when the mode number increases. When the FG index increases in both of linear and nonlinear loading factors, the amount of plates buckling load increases. For more information, when the nonlocal parameter or aspect ratio increases, the amount of plate's buckling load reduced whether in linear or nonlinear load factor.

References

- Aksencer, T. and Aydogdu, M. (2011), "Levy type solution method for vibration and buckling of nanoplates using nonlocal elasticity theory", *Physica E: Low-dimensional Syst. Nanostruct.*, **43**(4), 954-959.
- Analooei, H., Azhari, M. and Heidarpoor, A. (2013), "Elastic buckling and vibration analyses of orthotropic nanoplates using nonlocal continuum mechanics and spline finite strip method", *Appl. Math. Modelling*, **37**(10-11), 6703-6717.
- Ansari, R., Ashrafi, M., Pourashraf, T. and Sahmani, S. (2015a), "Vibration and buckling characteristics of functionally graded nanoplates subjected to thermal loading based on surface elasticity theory", *Acta Astronautica*, **109**, 42-51.
- Ansari, R., Shojaei, M.F., Shahabodini, A. and Bazdid-Vahdati, M. (2015b), "Three-dimensional bending and vibration analysis of functionally graded nanoplates by a novel differential quadrature-based approach", *Composite Struct.*, **131**, 753-764.
- Bedroud, M., Nazemnezhad, R. and Hosseini-Hashemi, S. (2015), "Axisymmetric/asymmetric buckling of functionally graded circular/annular Mindlin nanoplates via nonlocal elasticity", *Meccanica*, **50**(7), 1791-1806.
- Cheng, C.H. and Chen, T. (2015), "Size-dependent resonance and buckling behavior of nanoplates with high-order surface stress effects", *Physica E: Low-dimensional Syst. Nanostruct.*, **67**, 12-17.
- Daneshmehr, A., Rajabpoor, A. and Hadi, A. (2015), "Size dependent free vibration analysis of nanoplates made of functionally graded materials based on nonlocal elasticity theory with high order theories", *J. Eng. Sci.*, **95**, 23-35.
- Farajpour, A., Danesh, M. and Mohammadi, M. (2011), "Buckling analysis of variable thickness nanoplates using nonlocal continuum mechanics", *Physica E: Low-dimensional Syst. Nanostruct.*, **44**(3), 719-727.
- Farajpour, A., Shahidi, A., Mohammadi, M. and Mahzoon, M. (2012), "Buckling of orthotropic micro/nanoscale plates under linearly varying in-plane load via nonlocal continuum mechanics", *Composite Struct.*, **94**(5), 1605-1615.
- Li, L. and Hu, Y. (2017), "Torsional vibration of bi-directional functionally graded nanotubes based on nonlocal elasticity theory", *Composite Struct.*, **172**, 242-250.
- Li, L., Li, X. and Hu, Y. (2018), "Nonlinear bending of a two-dimensionally functionally graded beam", *Composite Struct.*, **184**, 1049-1061.
- Mori, T. and Tanaka, K. (1973), "Average stress in matrix and average elastic energy of materials with misfitting inclusions", *Acta Metallurgica*, **21**(5), 571-574.

- Naderi, A. and Saidi, A. (2013), "Modified nonlocal mindlin plate theory for buckling analysis of nanoplates", *J. Nanomech. Micromech.*, **4**(4), A4013015.
- Nami, M.R., Janghorban, M. and Damadam, M. (2015), "Thermal buckling analysis of functionally graded rectangular nanoplates based on nonlocal third-order shear deformation theory", *Aerosp. Sci. Technol.*, **41**, 7-15.
- Nguyen, N.T., Hui, D., Lee, J. and Nguyen-Xuan, H. (2015), "An efficient computational approach for size-dependent analysis of functionally graded nanoplates", *Comput. Methods Appl. Mech. Eng.*, **297**, 191-218.
- Park, J.S. and Kim, J.H. (2006), "Thermal postbuckling and vibration analyses of functionally graded plates", *J. Sound Vib.* **289**(1-2), 77-93.
- Pradhan, S. (2012), "Buckling analysis and small scale effect of biaxially compressed graphene sheets using non-local elasticity theory", *Sadhana*, **37**(4), 461-480.
- Pradhan, S. and Kumar, A. (2011), "Buckling analysis of single layered graphene sheet under biaxial compression using nonlocal elasticity theory and DQ method", *J. Comput. Theoretical Nanosci.*, **8**(7), 1325-1334.
- Pradhan, S. and Murmu, T. (2009), "Small scale effect on the buckling of single-layered graphene sheets under biaxial compression via nonlocal continuum mechanics", *Comput. Mater. Sci.*, **47**(1), 268-274.
- Pradhan, S. and Murmu, T. (2010). "Small scale effect on the buckling analysis of single-layered graphene sheet embedded in an elastic medium based on nonlocal plate theory", *Physica E: Low-dimensional Syst. Nanostruct.*, **42**(5), 1293-1301.
- Pradhan, S. and Phadikar, J. (2011), "Nonlocal theory for buckling of nanoplates", *J. Struct. Stability Dynam.*, **11**(3), 411-429.
- Salehipour, H., Nahvi, H. and Shahidi, A. (2015a), "Exact analytical solution for free vibration of functionally graded micro/nanoplates via three-dimensional nonlocal elasticity", *Physica E: Low-dimensional Syst. Nanostruct.*, **66**, 350-358.
- Salehipour, H., Nahvi, H. and Shahidi, A. (2015b), "Exact closed-form free vibration analysis for functionally graded micro/nano plates based on modified couple stress and three-dimensional elasticity theories", *Composite Struct.*, **124**, 283-291.
- Samaei, A., Abbasian, S. and Mirsayar, M. (2011), "Buckling analysis of a single-layer graphene sheet embedded in an elastic medium based on nonlocal Mindlin plate theory", *Mech. Res. Commun.*, **38**(7), 481-485.
- Zare, M., Nazemnezhad, R. and Hosseini-Hashemi, S. (2015), "Natural frequency analysis of functionally graded rectangular nanoplates with different boundary conditions via an analytical method", *Meccanica*, **50**(9), 2391-2408.
- Zhu, X. and Li, L. (2017a), "Twisting statics of functionally graded nanotubes using Eringen's nonlocal integral model", *Composite Struct.*, **178**, 87-96.
- Zhu, X. and Li, L. (2017b), "Longitudinal and torsional vibrations of size-dependent rods via nonlocal integral elasticity", *J. Mech. Sci.*, **133**, 639-650.
- Zhu, X. and Li, L. (2017c), "Closed form solution for a nonlocal strain gradient rod in tension", *J. Eng. Sci.*, **119**, 16-28.

